pentadienyl rings and the hydrogen atom on C19 of I were included with isotropic thermal parameters but were not allowed to vary. The central isopropoxide carbon atom, C19 of II, refined with anisotropic thermal parameters to a long ellipsoidal shaped atom, which strongly suggested disorder; this atom was assumed to be disordered and refined as two isotropic half-atoms. Scattering factors[19] were adjusted for anomalous dispersion. The positional parameters in Tables II and III, and crystal data are in Table IV.

(19) *International Tables for X-ray Crystallography*; Kynoch: Birmingham, England, 1974; Vol. IV.

Supplementary Material Available: Tables of thermal parameters, additional distances and angles, calculated hydrogen positions, and the least-squares planes (10 pages); listings of the observed structure factors (14 pages). Ordering information is given on any current masthead page.

Electronic Structure of Bis(dimethylmethylenephosphoranyl)dihydroborato(1–) Main-Group and Transition-Metal Complexes. A Case Study Involving Theoretical Pseudopotential ab Initio Calculations and UV Photoelectron Spectroscopy

Giovanni Bruno, Enrico Ciliberto, Santo Di Bella, and Ignazio Fragalà*

*Dipartimento di Scienze Chimiche, Università di Catania, 95125 Catania, Italy*

Gerhard Müller

Anorganisch-chemisches Institut, Technische Universität München, D-8046 Garching, Federal Republic of Germany

This contribution describes a study that uses He I/He II UV photoelectron spectroscopy and theoretical ab initio pseudopotential calculations to investigate the electronic structure of a large series of bis(dimethylmethylenephosphoranyl)dihydroborato(1–) [(L)⁻] complexes. The series includes the pseudotetrahedral complexes $(CH_3)_2M(L)$ (M = Al, Ga) and $M(L)_2$ (M = Be, Cd, Hg), as well as the square-planar $M(L)_2$ (M = Ni, Pd, Pt) complexes. All complexes represent unusual examples of tetracoordinated alkyls and, in the case of homoleptic $M(L)_2$ complexes of d^8 transition-metal M(II) ions (M = Ni, Pt, Pd), are almost unique examples of square-planar alkyls. Reorganization energies in the ionic state as well as relativistic corrections in the case of the heavy atom in the $Pt(L)_2$ complex have been taken into account to interpret the photoelectron spectra. The theoretical results provide a convincing description of the metal–ligand bonding in these complexes. In the case of the $(CH_3)_2M(L)$ complexes both theoretical and experimental results indicate that their uppermost MOs can be described in terms of symmetry combinations of the ligand ylidic and methyl lone pairs perturbed by the metal subshells. This is also true in the case of the group II metal complexes. The metal–ligand bonding appears much more intriguing in the square-planar d^8 metal complexes, in which the metal d subshells lead to severe perturbations not only of ligand ylidic lone pairs but also of the deep σ MOs. Detailed assignments of the photoelectron spectra are proposed on the basis of both theoretical and experimental results. A tentative comparison of bonding between the phosphorus ylide under study and the more usual hydrocarbyl complexes has been carried out.

Introduction

In recent years the bis(dimethylmethylenephosphoranyl)dihydroborate uninegative anion [(L)⁻] has been recognized as a novel, powerful ligand (I).[1] It has proven capable of stabilizing stoichiometries and coordination environments uncommon within usual homoleptic hydrocarbyls, thus forming stable metal-to-carbon σ-bonds with almost all the metals of the periodic table.[1] These,
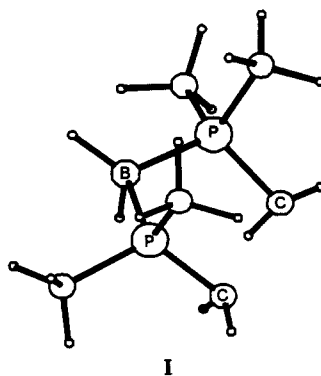
(1) (a) Schmidbaur, H. *Acc. Chem. Res.* **1975**, *8*, 62. (b) Schmidbaur, H. *Pure Appl. Chem.* **1978**, *50*, 19; **1980**, *52*, 1057. (c) Schmidbaur, H. *J. Organomet. Chem.* **1980**, *200*, 287. (d) Schmidbaur, H. *ACS Symp. Ser.* **1981**, *No. 171*, 87. (e) Schmidbaur, H. In *Transition Metal Chemistry: Current Problems*; Müller, A., Diemann, E., Eds.; Verlag Chemie: Weinheim, Germany 1981; p 107. (f) Schmidbaur, H. *Angew. Chem., Int. Ed. Engl.* **1983**, *22*, 907. (g) Kaska, W. C. *Coord. Chem. Rev.* **1983**, *48*, 1.

I

so called "onium-stabilized alkyls" possess equivalent Me_2PCH_2 groups and, hence, symmetrical bonding of lig-

ands to the metal centers. The geometry of the ligand skeleton changes very little upon complexation, so that the resulting metal complexes contain essentially strain-free six-membered rings in a chair conformation.[2] Steric and inductive effects due to the phosphonium centers seem to be the source of the stabilities of the resulting neutral, monomeric complexes especially in the case of coordinated metals having coordination architecture not encountered among other hydrocarbyls.[2]

Almost all these complexes possess remarkable thermal stabilities. They also have reasonable vapor pressures in the 80–120 °C temperature range.[2a,b] They therefore lend themselves to study by gas-phase photoelectron (PE) spectroscopy.

In this paper, a case study is reported of the electronic structure of a wide series of complexes of the title ligand with various main-group and transition-metal ions. The compounds studied include pseudotetrahedral complexes $(CH_3)_2M(L)$ (M = Al, Ga) and $M(L)_2$ (M = Be, Cd, Hg) and square-planar complexes $M(L)_2$ (M = Ni, Pd, Pt). This study combines accurate pseudopotential ab initio calculations[3] of complexes representative of each series, and the evaluation of ionization energies (IEs) through ΔSCF calculations with the experimental He I/He II PE spectra.[3]

All the complexes studied represent unusual examples of tetracoordinated alkyls and, in the case of homoleptic $M(L)_2$ complexes of d^8 transition metal M^{II} ions (M = Ni, Pt, Pd), are almost unique examples of square-planar alkyls.

Experimental Section

The preparative routes to complexes $[(CH_3)_2M(L)$ (M = Al, and Ga) and $M(L)_2$ (M = Be, Cd, Hg, Ni, Pd, Pt)] have already been reported.[2]

These compounds were always handled under prepurified molecular nitrogen. Prior to PE measurements each complex was purified by sublimation in vacuo. Previous mass spectral measurements for some of the complexes studied have shown the presence of monomeric species in the gas-phase above the heated solid.[1c,2] The $Hg(L)_2$ complex exhibited some thermal lability.

Photoelectron Spectroscopy. PE spectra were recorded with the aid of a photoelectron spectrometer interfaced to an IBM PC AT computer as described elsewhere.[3,4] Procedures used to "lock" the energy scale to defined internal references were used, and these have also been described previously.[3,4] Spectral resolution measured for the Ar^+ $^2P_{3/2}$ component was always better than 0.045 eV. Deconvoluted He II spectra were corrected only for the He IIβ "satellite" contributions (11% of the reference N_2 spectrum under operating conditions). The procedures used for spectral deconvolution have been described elsewhere ($R \leq 0.04$).[3,4,5]

Computational Details. Pseudopotential LCAO-MO-SCF calculations were carried out at the ab initio level[6] using the PSHONDO program.[7] Pseudopotential literature parameters were

used.[8] In the case the Pt complex, the metal pseudopotential[9] included the major relativistic (mass and Darwin) corrections.[10,11] Valence basis sets were of double-ζ quality as described elsewhere.[3] A d-polarization function (ζ = 0.45) was used on each P atom.[14] Gross atomic charges and bond overlap populations were computed.[3,4] Also the procedures used for the evaluation of ionization energies have been reported elsewhere.[3,4]

The geometrical parameters taken for the anionic ligand were averaged from those known for the various (L)⁻ complexes[1c] and constrained to a C_s symmetry. Structures of the $(CH_3)_2M(L)$ (M = Al, Ga) complexes are, however, not known. There is, however, an indication that their geometries are similar to those of the analogous complexes of the closely related ligand methanide bis(dimethylphosphonium methylide).[1c] Therefore geometrical parameters of $(CH_3)_2Al(L)$ were adapted from the available X-ray data of both the Ga complex of the above closely related ligand[17] and of $Al_2(CH_3)_6$,[18] (Al–C_{meth} = 1.98 Å and Al–C_{yl} = 2.08 Å). A C_s symmetry was also assumed for $(CH_3)_2Al(L)$. Parameters used for the Pd and Pt complexes were adapted from available X-ray data of the Ni complex,[2b] assuming a C_{2h} symmetry. This is reasonable since similar structures are expected along the series.[1c,2b] The Pd–C and Pt–C distances, taken as 2.02 and 2.08 Å for $Pd(L)_2$ and $Pt(L)_2$, respectively, were deduced from the average Pd–C and Pt–C distances found in other ylide[19] and alkyl[20] complexes. The coordinate system used is shown in Figure 7. Calculations were always made for model compounds where the –$P(CH_3)_2$ groups have been replaced by –PH_2 units.

Results and Discussion

Bis(dimethylmethylenephosphoranyl)dihydroborate(1–) Anion Ligand. In accordance with the synthetic route,[1c] the discussion of the electronic structure of

(2) (a) Schmidbaur, H.; Müller, G.; Schubert, U.; Orama, O. *Angew. Chem.* **1978**, *90*, 126; *Angew. Chem., Int. Ed. Engl.* **1978**, *17*, 126. (b) Müller, G.; Schubert, U.; Orama, O.; Schmidbaur, H. *Chem. Ber.* **1979**, *112*, 3302. (c) Schmidbaur, H.; Füller, H.-J.; Müller, G.; Frank, A. *Chem. Ber.* **1979**, *112*, 1448. (d) Müller, G. Dissertation, Technical University of Munich, 1980. (e) Schmidbaur, H.; Müller, G. *Monatsh. Chem.* **1980**, *111*, 1233. (f) Schmidbaur, H.; Müller, G.; Dash, K. C.; Milewski-Mahrla, B. *Chem. Ber.* **1981**, *114*, 441. (g) Müller, G.; Neugebauer, D.; Geike, W.; Köhler, F. H.; Pebler, J.; Schmidbaur, H. *Organometallics* **1983**, *2*, 257.

(3) (a) Di Bella, S.; Fragalà, I.; Granozzi, G. *Inorg. Chem.* **1986**, *25*, 3997, and references therein. (b) Di Bella, S.; Casarin, M.; Fragalà, I.; Granozzi, G.; Marks, T. J. *Inorg. Chem.* **1988**, *27*, 3993.

(4) Di Bella, S. Ph.D. Thesis, University of Catania, 1986.

(5) Casarin, M.; Ciliberto, E.; Gulino, A.; Fragalà, I. *Organometallics* **1989**, *8*, 900.

(6) (a) Durand, Ph.; Barthelat, J. C. *Theor. Chim. Acta* **1975**, *38*, 283. (b) Barthelat, J. C.; Durand, Ph.; Serafini, A. *Mol. Phys.* **1977**, *33*, 159. (c) Pélissier, M.; Durand, Ph. *Theor. Chim. Acta* **1980**, *55*, 43.

(7) Pseudopotential adaptation (Daudey, J. P.) of HONDO 76: Dupuis, M.; Rys, J.; King, H. F. *QCPE* **1977**, *11*, 338.

(8) (a) *Molecular ab initio Calculations Using Pseudopotentials*; Technical Report, Laboratoire de Physique Quantique, Toulouse, 1981. (b) Daudey, J. P.; Jeung, G.; Ruiz, M. E.; Novaro, O. *Mol. Phys.* **1982**, *46*, 67.

(9) Daudey, J. P., private communication.

(10) Barthelat, J. C.; Pélissier, M.; Durand, Ph. *Phys. Rev. A* **1980**, *21*, 1773.

(11) The effect of spin-orbit coupling has not been explicitly taken into account since the absence of degenerate levels prevents (Kramer's theorem) the observation of a greater number of ion states than that of ground-state MOs. Furthermore, it is well-known that off-diagonal mixing in the corresponding double group due to the so-called "induced or indirect spin-orbit effect"[12] is of minor relevance in square-planar Pt^{II} complexes.[13]

(12) (a) Pyykkö, P. *Adv. Quantum Chem.* **1978**, *11*, 353. (b) Snijders, J. G.; Baerends, E.; Ros, P. *Mol. Phys.* **1979**, *38*, 1909.

(13) See for example: (a) Hay, P. J. *J. Am. Chem. Soc.* **1981**, *103*, 1390. (b) Louwen, J. N.; Hengelmolen, R.; Grove, D. M.; Oskam, A.; DeKock, R. L. *Organometallics* **1984**, *3*, 908. (c) Louwen, J. N.; Hengelmolen, R.; Grove, D. M.; Stufkens, D. J.; Oskam, A. *J. Chem. Soc., Dalton Trans.* **1986**, 141.

(14) d-polarization functions allows a better description of the ylidic electronic system[15] since the negative charge over the ligand appears better averaged on both P and C atoms (see Table I). Nevertheless, there is an indication that they are not crucial to describe π acceptor properties of phosphorus atoms,[16] and furthermore, only negligible changes (see Table I) of ground-state eigenvalues and eigenvectors seem to be due to their use. Therefore no such functions have been used for calculations of metal complexes in order to save considerable computational efforts.

(15) See for example: (a) Absar, I.; Van Wazer, J. R. *J. Am. Chem. Soc.* **1972**, *94*, 2382. (b) Ostoja-Starzewski, K. A.; Tom Dieck, H.; Bock, H. *J. Organomet. Chem.* **1974**, *65*, 311. (c) Ostoja-Starzewski, K. A.; Bock, H. *J. Am. Chem. Soc.* **1976**, *98*, 8486. (d) Mitchell, D. J.; Wolfe, S.; Schlegel, H. B. *Can. J. Chem.* **1981**, *59*, 3280. (e) Yates, B. F.; Bouma, W. J.; Radom, L. *J. Am. Chem. Soc.* **1987**, *109*, 2250.

(16) Xiao, S.-X.; Trogler, W. C.; Ellis, D. E.; Berkovitch-Yellin, Z. *J. Am. Chem. Soc.* **1983**, *105*, 7033.

(17) Schmidbaur, H.; Gasser, O.; Krüger, C.; Sekutowski, J. C. *Chem. Ber.* **1977**, *110*, 3517.

(18) (a) Moore, J. W.; Sanders, D. A.; Scherr, P. A.; Glick, M. D.; Oliver, J. P. *J. Am. Chem. Soc.* **1971**, *93*, 1035. (b) Albright, M. J.; Butler, W. M.; Anderson, T. J.; Glick, M. D.; Oliver, J. P. *J. Am. Chem. Soc.* **1976**, *98*, 3995.

(19) Weber, L. In *The Chemistry of the Metal–Carbon Bond*; Hartley, F. R., Patai, S., Eds.; Wiley: New York, 1982; Chapter 3.

(20) Harthey, F. R. In *Comprehensive Organometallic Chemistry*; Wilkinson, G., Stone, F. G. A., Abel, E. W., Eds.; Pergamon: Oxford, 1982; Chapter 39.5.

Table I. Ab Initio Eigenvalues and Population Analysis of Outermost MOs of the model ligand (L)⁻

| MO | eigenvalue,[a] eV | population,[a] % | | | | | | character |
		C	P	B	H_C	H_P	H_B	
7a″	0.52 (0.79)	83 (81)	6 (12)		2	9 (7)		n_-
9a′	2.65 (2.88)	84 (81)	3 (9)	2 (2)	2 (1)	9 (7)		n_+
8a′	6.64 (6.49)	3 (5)	29 (32)	31 (31)	1 (1)	10 (8)	26 (23)	σ_+(P–B)
6a″	7.38 (7.12)	9 (9)	57 (58)	23 (23)	5 (5)	6 (5)		σ_-(P–B)
7a′	7.44 (7.48)	21 (19)	23 (21)	18 (17)	7 (8)	10 (10)	21 (25)	σ_+(P–C)
5a″	7.98 (7.96)	31 (30)	35 (36)	1 (1)	17 (16)	16 (16)		σ_-(P–C)

Atomic Charge[a]

C	P	B	H_C	H_P	H_B
−0.300 (−0.165)	−0.008 (−0.191)	+0.144 (+0.262)	−0.044 (−0.064)	−0.033 (−0.001)	−0.110 (−0.145)

Overlap Population[a]

P–C	P–B
0.940 (1.090)	0.440 (0.536)

[a] Values in parentheses refer to calculation including 3d polarization functions on the phosphorus atoms.

the anion ligand is, perhaps, best based upon that of the trimethylphosphine–borane precursor.[21] Within a qualitative localized-bond model its valence electronic structure in C_{3v} symmetry, consists of (i) the 4e and 5e orbitals featuring respectively the P–C and B–H bond of local π symmetry, (ii) the $5a_1$ orbital, which comprises the σ P–B bond, and finally (iii) the 6e and $6a_1$ orbitals, which are the virtual antibonding counterparts of 4e and $5a_1$ orbitals, respectively. A nest of σ orbitals composed of C–H bonds is situated somewhat deeper (Figure 1a).

Hydride abstraction results in the π-acid $((CH_3)_3PBH_2)^+$ cation[22] of C_s symmetry and involves a major perturbation of the doubly degenerate 5e orbitals. Of these two, the $\pi_x{}^{24}$ is found in the destabilized 9a′ (C_s) LUMO orbital (Figure 1b), which has a dominant B_{2p} character. The remaining $\pi_y{}^{24}$ orbital undergoes energy stabilization (5a″) because of both the positive charge and a mechanism strongly reminiscent of Jahn–Teller distortion.[25] Smaller energy stabilizations must be expected for almost all the remaining valence orbitals because of the positive charge.

The reaction pathway to the dihydrobis(trimethylphosphane)boron(1+) cation involves interaction between the P_{3p} lone pair orbital (which is a_1 in a local C_{3v} symmetry) of the incoming $P(CH_3)_3$ molecule[16] and the 9a′ LUMO of the precursor cation, thus resulting in the empty 14a″ orbital and in the filled 13a″ orbitals (Figure 1c). The latter formally represents the new P–B bond. The other orbitals of the precursor molecule, with the exception only of those representing B–H bonds, are degenerate in the symmetrical cation due to the operation of symmetry elements of the C_s point group.

Functionalization of the methyl groups results in the ylide anion (L)⁻ whose electronic structure follows necessarily from that of the (trimethylphosphane)boron cation once it is considered that proton abstraction, and hence attainment of the ylidic structure, results in (i) a major destabilization of two suitable orbitals from the σ C–H manifold thus giving new orbitals formally describing the in-the-phase and out-of-phase combinations of the ylidic lone pairs (hereafter n_+, n_-) and (ii) less remarkable changes in the nature and the energy of the remaining valence orbitals (Figure 1d).
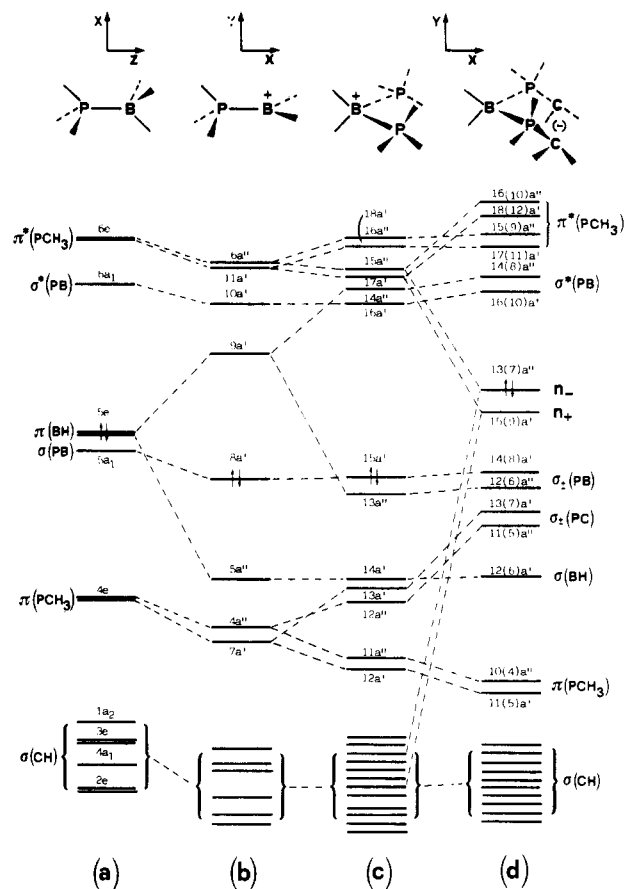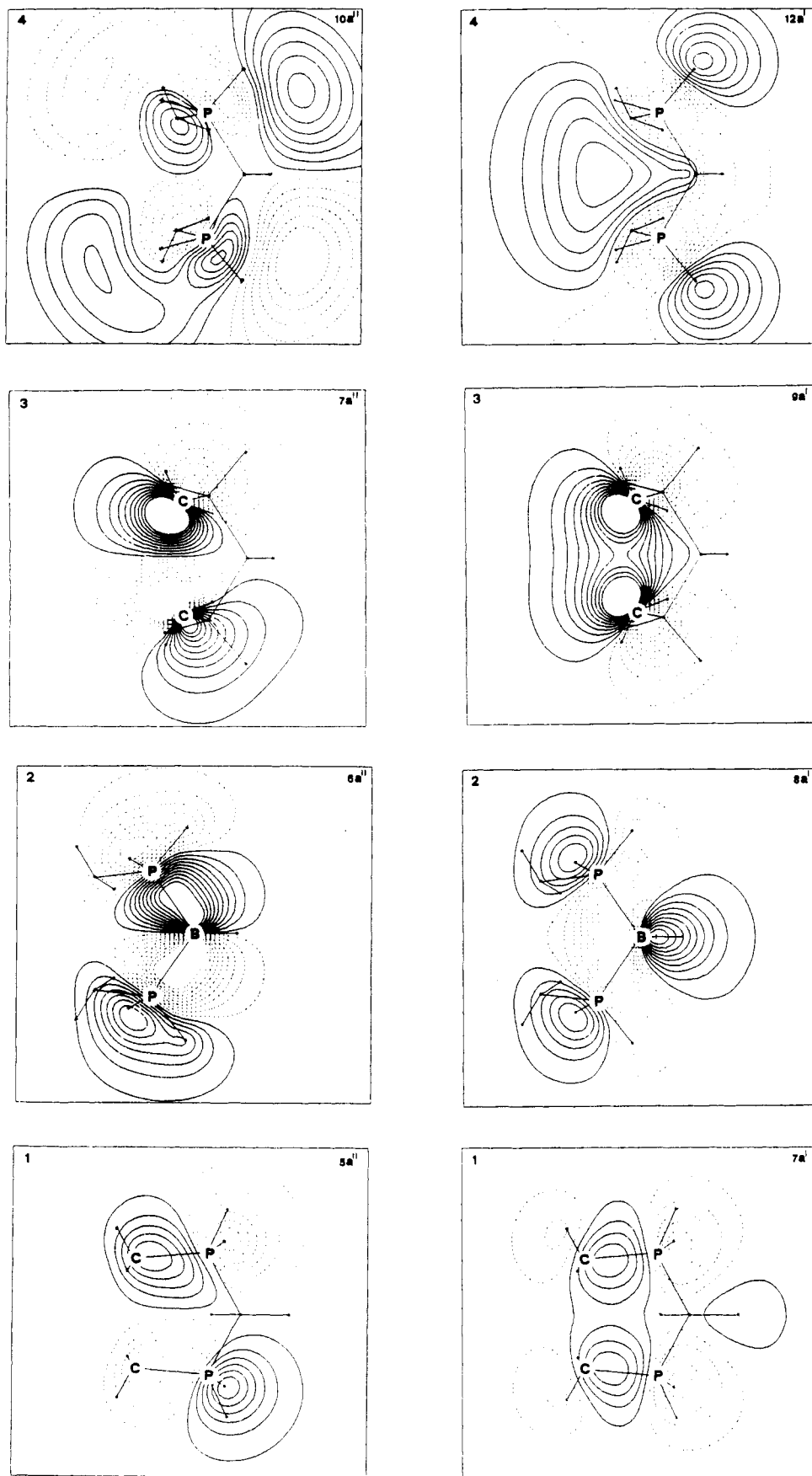
(21) (a) Hillier, I. H.; Saunders, V. R. *J. Chem. Soc. A* 1971, 664. (b) Cowley, A. H.; Kemp. R. A.; Lattman, M.; McKee, M. L. *Inorg. Chem.* 1982, *21*, 85.
(22) The $((CH_3)_3PBH_2)^+$ cation is formally analogous to a $(AH_3BH_2)^+$ system. See ref 23, Chapter 10.
(23) Albright, T. A.; Burdett, J. K.; Whangbo, M.-H. *Orbital Interactions in Chemistry*; Wiley: New York; 1985.
(24) The notation refers to that adopted in ref 23.
(25) See for example ref 23, p 95.

Figure 1. Correlation diagram between qualitative MO levels of $(CH_3)_3PBH_3$ (a), $((CH_3)_3PBH_2)^+$ (b), $(((CH_3)_3P)_2BH_2)^+$ (c), and (L)⁻ (d). Numbering of various MOs relates to electron counting including methyl groups. Values in parentheses refer to the model compound.

The computed ab initio wave functions for the model (L)⁻ anion are in good agreement with such a qualitative description. Population data (Table I) and contour plots (Figure 2) of the outermost molecular orbitals (MOs) support correlation arguments outlined in Figure 1. In this context, it is worthy of note that contour plots in suitable planes of virtual π^*(P–H) (12a′, 10a″) orbitals of the model anion (Figure 2) show that they can overlap in a π fashion with ylidic lone pairs because of the chair conformation.[1c] This means that as long as the methyl functionalization occurs, the ylidic lone pairs are involved in a two-electron stabilizing interaction[15d] which represents a considerable source of stability of the ylide structure.[15d,26]

Figure 2. Wave function contour plots of the model (L)⁻ for the 5a″ (σ_-(P–C)), 7a′ (σ_+(P–C)), 6a″ (σ_-(P–B)), 8a′ (σ_+(P–B)), 7a″ (n_-), 9a′ (n_+), 10a″ (π^*(P–H)), and 12a′ (π^*(P–H)) MOs: view 1, xz plane through P–C bonds; view 2, xz plane through P–B–C bond; view 3, xz plane through the C atoms; view 4, parallel to view 3 plane through PH₂ bonds. Each set of contours is drawn in a frame of 8 × 8 au, and the stars indicate projections of each atom on the contour plane. The first solid and point contours are ±0.133 $e^{1/2}$/au³/² respectively, and the interval between successive contours is 0.014 $e^{1/2}$/au³/². The point lines refer to the negative part of the wave function.

Table II. Ab Initio Eigenvalues and Population Analysis of Outermost MOs of the Model $(CH_3)_2Al(L)$

MO	eigenvalue, eV	Al 3s	Al 3p	C_{yl}	C_{meth}	P	B	H_{yl}	H_{meth}	H_P	H_B	character
15a′	−9.17		17		76				7			n_-(meth), p_y
14a′	−9.58		12	32	44	3	1		8			n_+, p_x
9a″	−9.95		7	76	2	5	4	3		3		n_-(yl), p_z
13a′	−11.39			4		25	32			13	26	σ_+(P–B)
8a″	−12.61			17	5	53	19	4		2		σ_-(P–B)
12a′	−12.63	1		20	5	13	28	3		4	26	σ (B–H)
11a′	−13.33		1		51				48			σ (CH_3)
7a″	−13.39			2	51	1			46			σ (CH_3)
10a′	−13.54	17		33	25	4	4	3	7	2	5	n_+, s

Atomic Charge[a]

Al	C_{yl}	C_{meth}	P	B
+1.351	−0.599	−0.771	+0.023	+0.123

Overlap Population[a]

Al-C_{yl}	Al-C_{meth}	P-C_{yl}	P-B
0.342	0.372	0.596	0.400

[a] yl = ylidic; meth = methylic.

PE Spectra of the Main Group III Metal Complexes.

The $(CH_3)_2M(L)$ complexes (M = Al, Ga) possess a pseudotetrahedral geometry (II).[1c] Table II presents
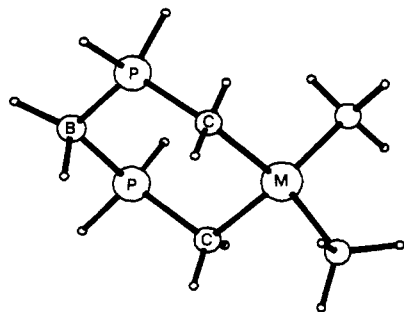
II

relevant ab initio data of the model $(CH_3)_2Al(L)$ complex. Population analysis of the outermost MOs indicates that the metal–ligand bonding involves only MOs having either dominant C-ylidic or C-methyl character. In particular, the 15a′ and 9a″ MOs are due to interactions of the out-of-phase combination of methyl and of ylidic lone pairs with the $3p_y$ and $3p_z$ metal orbitals (Figure 3). The 14a′ and 10a′ MOs are locally out-of-phase and in-phase combinations of methyl and ylidic lone pairs mediated by the metal $3p_x$ and 3s orbitals, respectively (Figure 3). Interestingly enough, the nodal properties as well as the energy grouping (Table II) of these four MOs are very similar to those of MOs representing combinations of σ(M–C) bonds (t_2 and a_1) in a classical metal tetramethyl complex of T_d symmetry.[27] They are the major source of the metal–ligand bonding and mainly responsible for a significant ligand–metal charge transfer leading to a charge on the metal center of +1.351 (Table II). The remaining orbitals are almost totally ligand-based, unperturbed MOs.

The photoelectron spectra of $(CH_3)_2M(L)$ (M = Al and Ga) are very similar to each other (Figure 4). They show a well-resolved band, band a, in the region up to 9.5-eV IE. The higher IE region consists of an ill-resolved band, band b, around 10 eV and of strongly overlapping struc-

Table III. Experimental IEs, Computed IEs, and Assignments of the PE Spectra of $(CH_3)_2Al(L)$ and $(CH_3)_2Ga(L)$ Complexes

band label	$(CH_3)_2Al(L)$ exptl	ΔSCF	PT[a]	$(CH_3)_2Ga(L)$ exptl IE, eV	assgnt
a	8.76 (0.54)[b]	7.98 / 8.73 / 8.96	7.99 / 8.71 / 8.91	8.30 (0.58)[b]	15′ / 14a′ / 9a″ } σ(M–C)
b	10.34		10.51 / 11.82	10.19	13a′ / 8a″ } $\sigma_\pm$(P–B)
c	12.27			12.17	inner σ
d	14.13			14.05	inner σ
x				23.60	"$^2D_{5/2}$"
x′				23.99	"$^2D_{3/2}$"

[a] PT = perturbative treatment (see for instance ref 3). [b] Half-width.

tures, bands c and d, in the region up to 17 eV. A remarkable depression of band b is observed in the He II spectra (Figure 4) together with new features, in the 23–25-eV region, which are not accessible by He I radiation. Notably, the He II spectrum of the Ga complex shows a clearly distinct band, band x (∼24 eV), which has no counterpart in the spectrum of the Al homologue.

ΔSCF ab initio IE values provide a reliable rationale of the PE spectra (Table III). Band a must be associated with ionization from the 15a′, 14a′, and 9a″ MOs. the ΔSCF IE spread agrees well with the experimental band half-width (Table III).

The assignment of band b poses some problems since calculations would suggest the assignment to ionization of the 13a′ (σ_+(P–B)) MO. However the theoretical calculations refer to a model compound without methyl groups on the phosphorus atoms. Therefore, the ionization of the 8a″ MO, having significant amplitudes on the phosphorus atoms (Table II), must be expected at lower IE than the computed value.[21b] Band b, therefore, might encompass ionization of the 8a″ (σ_-(P–B)) MO as well and, in any case, the smaller intensity observed in the He II spectrum agrees well with the dominant P_{3p} and B_{2p} character[28] of both the mentioned MOs.

The spectral features in the higher IE region belong to ionization of inner σ and π MOs and certainly include the

(26) See also ref 23, p 171.

(27) See for example: (a) Evans, S.; Green, J. C.; Joachim, P. J.; Orchard, A. F.; Turner, D. W.; Maier, J. P. *J. Chem. Soc., Faraday Trans. 2* **1972**, *68*, 905. (b) Ballard, R. E. *Photoelectron Spectroscopy and Molecular Orbital Theory*; Hilger: Bristol, 1978; Chapter 9.
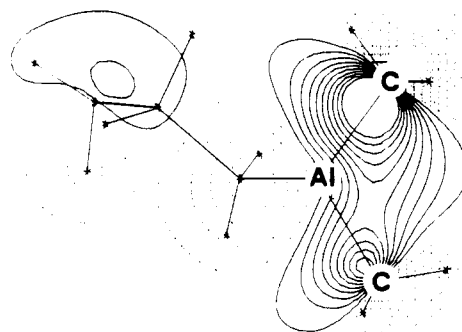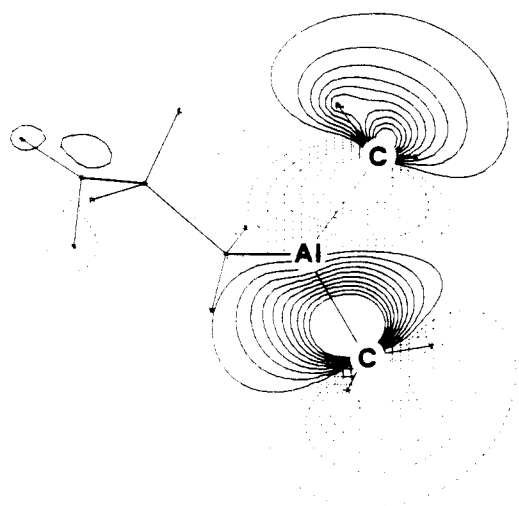
(28) Rabalais, J. W. *Principles of Ultraviolet Photoelectron Spectroscopy*; Wiley: New York, 1977; p 335.
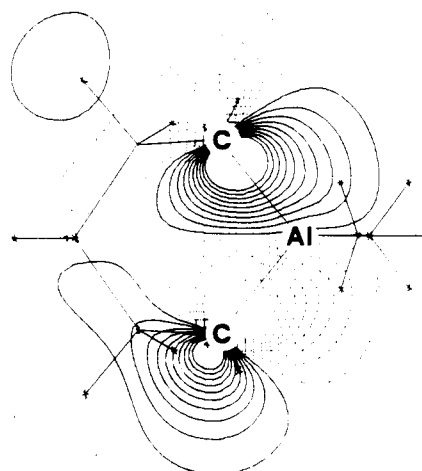
2

15a'

2

14a'

1

10a'

1

9a''

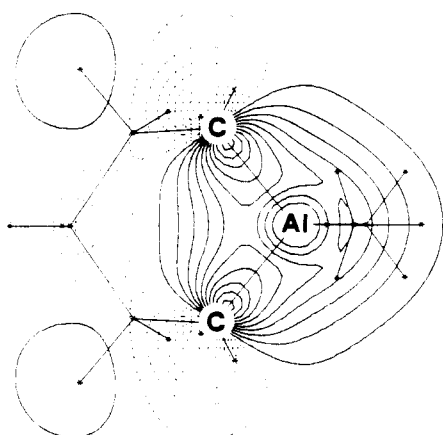**Figure 3.** Wave function contour plots of the model $(CH_3)_2Al(L)$ for the 9a'', 10a', 14a', and 15a' MOs: view 1, xz plane through C_{yl}–Al–C_{yl} bond; view 2, xy plane through C_{meth}–Al–C_{meth} bond. Each set of contours is drawn in a frame of 10 × 10 au and the stars indicate projections of each atom on the contour plane. Contours interval as in Figure 2.

Table IV. Experimental IEs (eV) and Assignments of the PE Spectra of $M(L)_2$ (M = Be, Cd, Hg) Complexes

| band label | IE, eV | | | assignt |
	Be(L)₂	Cd(L)₂	Hg(L)₂	
a	7.68 (0.58)[a]	7.03 (0.56)[a]	6.96 (1.90)[b]	σ(M–C)
a'			7.52 (1.10)[b] (0.57)[a]	σ(M–C)
b'	9.75 (sh)	9.50 (sh)	9.81 (sh)	$\sigma_{\pm}$(P–B)
b	10.35	10.17	10.42	$\sigma_{\pm}$(P–B)
c	11.90	11.71	11.65	inner σ
d	13.82	13.60	13.70	inner σ

[a] Half-width. [b] Relative intensity of components a and a' in the He I spectrum.

10a' MO. Nevertheless their diffuse, overlapping nature precludes any detailed assignment.

Incidentally, it should be noted that the above general assignment is consistent with the assignments proposed for both the PE spectra of Al^{III} and Ga^{III} trimethyl complexes[29] and for the PE spectrum of trimethylphosphine–borane.[21b,30]

Finally, the higher IE structure (x in Figure 4) apparent in the He II spectrum of the Ga complex is considered.

The absence of an analogous band in the spectrum of the corresponding Al complex suggests assignment of this band to ionizations of "corelike" 3d^{10} orbitals.[31] As a matter of fact, the presence of two components in this band separated by 0.39 eV is consistent with spin–orbit coupling effects observed on ionization of 3d orbitals in the Ga atom[32] and in the (3d)$^{-1}$ ionization of Ga^{III} complexes.[31b]

(29) Barker, G. K.; Lappert, M. L.; Pedley, J. B.; Sharp, G. J.; Westwood, N. P. C. *J. Chem. Soc., Dalton Trans.* **1975**, 1765.
(30) Bock, H. *Pure Appl. Chem.* **1975**, 44, 343.

(31) (a) Berkowitz, J. *J. Chem. Phys.* **1974**, 61, 407. (b) Bancroff, G. M.; Coatsworth, L. L.; Creber, D. K.; Tse, J. *Chem. Phys. Lett.* **1977**, 50, 228.
(32) Carlson, T. A. *Photoelectron and Auger Spectroscopy*; Plenum: New York, 1975; p 337.
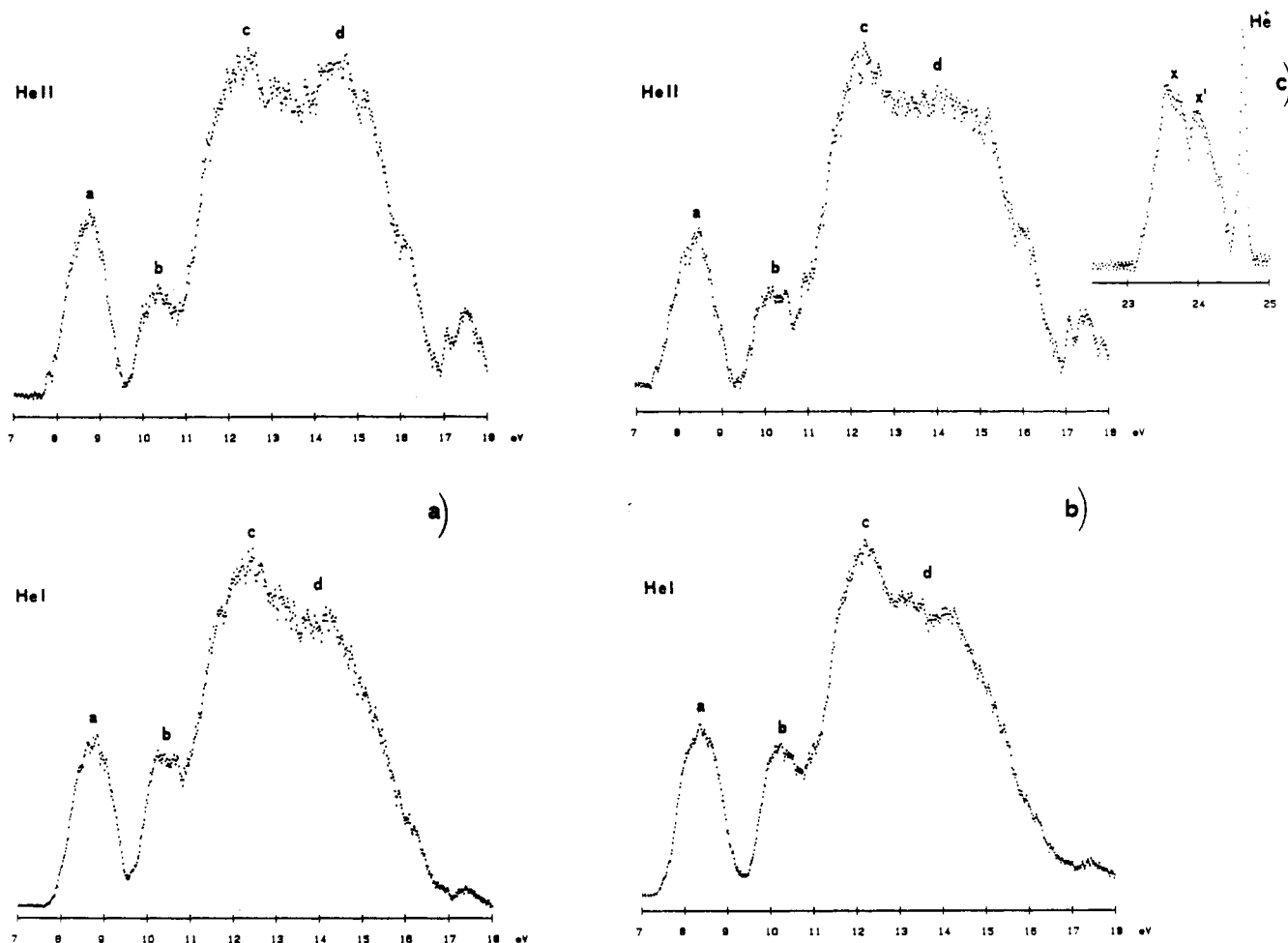
Figure 4. He I and He II PE spectra of $(CH_3)_2Al(L)$ (a), and $(CH_3)_2Ga(L)$ (b); He II PE spectrum of $(CH_3)_2Ga(L)$ (c) in the higher IE region.

PE Spectra of Group II Complexes. The $M(L)_2$ complexes (M = Be, Cd, Hg) possess a pseudotetrahedral ligand arrangement.[1c,2] Their He I and He II PE spectra are very similar to each other (Table IV) and closely resemble those of previous $(CH_3)_2M(L)$ complexes. Some differences, however, are noted: band b splits into two components, b' and b, and bands c and d, in the higher IE region, are differently structured. Relevant PE data are collected in Table IV. Spectra of the prototype $Be(L)_2$ are presented in Figure 5a.

The assignment of the low-IE features can be achieved using a localized bonding scheme based on simple overlap arguments.[33] There is evidence[33,34] (see also Table II) that the valence electronic structure of main-group complexes consists of suitable symmetry combinations of upper lying ligand MOs perturbed, to various extents, by interaction with metal *ns* and *np* subshells.

The group overlaps[33] ($G(M-L)$) of each relevant symmetry combination in D_{2d} symmetry of ligand MOs are listed in Table V. They lead to the qualitative interaction diagram pictured in Figure 6.

Therefore the onset of band a in the Be and Cd complexes is assigned to ionization of the $e + b_2$ ($\sigma(M-C)$) MOs. This band, in fact, splits into two components, a and a' in the PE spectrum of $Hg(L)_2$ (Figure 5b), which show

(33) Evans, S.; Hamnett, A.; Orchard, A. F.; Lloyd, D. R. *Faraday Discuss. Chem. Soc.* **1972**, *54*, 227.

(34) See for example: Bruno, G.; Ciliberto, E.; Fragalà, I.; Granozzi, G. *Inorg. Chim. Acta* **1980**, *48*, 61. Bruno, G.; Centineo, G.; Ciliberto, E.; Fragalà, I. *J. Electron Spectrosc. Relat. Phenom.* **1983**, *32*, 153.

Table V. Group Overlap Integrals Between Metal Valence AOs and Leading Ligand Symmetry Orbitals for the $M(L)_2$ (M = Be, Cd, Hg) Complexes

ligand orbital sym combination	metal orbital	$G(M-L)^a$
a_1 (n_+)	s	$\sqrt{2}S(s,p_\sigma)$
b_2 (n_+)	p_z	$S(p_\sigma,p_\sigma) + S(p_\pi,p_\pi)$
e (n_-)	p_x, p_y	$1/\sqrt{2}S(p_\sigma,p_\sigma) - 1/\sqrt{2}S(p_\pi,p_\pi)$

$^a S(p_\sigma,p_\sigma) = \langle M_{p\sigma}|C_{p\sigma}\rangle$; $S(p_\pi,p_\pi) = \langle M_{p\pi}|C_{p\pi}\rangle$.

a 2:1 intensity ratio (Table IV). In the former complexes there is no evidence of any splitting. Nevertheless, the constant band half-width observed on traversing the series (Table IV) is a clear indication of the general validity of the proposed assignment.

Bands b' and b likely represent ionization of more internal $\sigma_\pm(P-B)$ MOs. This assignment is again consistent with the dramatic falloff of intensities of the two structures under the more energetic He II radiation (Figure 5a; vide supra). The unresolved nature of the higher bands precludes any detailed assignment. The ionization of the totally symmetric a_1 $\sigma(M-C)$ combination is not clearly apparent.

PE Spectra of the d^8 Transition Metals. Nickel-triad d^8 ions form low-spin $M(L)_2$ complexes having a local ligand array of square-planar symmetry (Figure 7). The complexes are chemically and thermally stable in the order Ni < Pt < Pd.[2b] Results of ab initio ground-state calculations of the model $Pd(L)_2$ complex are compiled in Table VI and pictorially described in the qualitative interaction

Table VI. Ab Initio Eigenvalues and Population Analysis of Outermost MOs of the Model Pd(L)₂

MO	eigenvalue, eV	population, % Pd 4d	Pd 5s	Pd 5p	C	P	B	H_C	H_p	H_B	overlap popn Pd-C	dominant character
7a$_u$	7.52			9	78	3		2	8		0.076	n_-
9b$_u$	7.65			10	77	2	2	2	7		0.084	n_+
12a$_g$	7.82	48	19		20	5	1	2	5		0.012	d_{z^2}, n_+
11a$_g$	9.91	77			5	10	2	3	3		−0.012	d_{xz}, σ_+(P−C)
8b$_g$	9.96	80			3	11	1	2	3		0.000	d_{yz}, σ_-(P−C)
10a$_g$	10.84	58			4	9	9	9	4	7	−0.004	$d_{x^2-y^2}$, σ_+(P−B)
9a$_g$	11.02	28			1	17	24	2	8	20	0.010	σ_+(P−B), $d_{x^2-y^2}$
8b$_u$	11.04				1	25	32		12	30	0.000	σ_+(P−B)
7b$_g$	11.77	15			16	36	14	3	16		0.040	σ_-(P−B), d_{xy}
6a$_u$	12.04				7	60	24	2	7		0.000	σ_-(P−B)
7b$_u$	12.19				19	15	31	4	5	26	0.000	σ_+(P−C)
8a$_g$	12.43	25			23	8	24		2	18	0.024	σ_+(P−C), d_{xz} (39%), $d_{x^2-y^2}$ (35%), d_{z^2} (26%)
6b$_g$	12.49	28			34	25	8	2	3		0.070	n_-, d_{xy}
7a$_g$	12.73	32			33	4	9	4	8	10	0.035	d_{z^2}, n_+
5a$_u$	13.22				34	36		13	17		0.000	σ_-(P−C)
5b$_g$	13.60	11			29	30		10	20		0.018	σ_-(P−C), d_{yz}

Atomic Charge

Pd	C	P	B
+0.131	−0.226	+0.030	+0.102

Overlap Population

Pd−C	P−C	P−B
0.496	0.656	0.410

Metal Orbital Population

5s	5p$_x$	5p$_y$	5p$_z$	4d$_{x^2-y^2}$	4d$_{z^2}$	4d$_{xy}$	4d$_{xz}$	4d$_{yz}$
0.506	0.329	0.341	0.022	1.931	1.867	0.963	1.963	1.948

diagram presented in Figure 8.[35] Interaction involving filled metal 4d$_{z^2}$ and ligand 9a$_g$ (n_+) orbitals (Figure 8) results in the bonding and antibonding partners the 7a$_g$ and 12a$_g$ MOs (Figure 9). The latter has an associated positive Pd−C overlap population because of additional admixture with the empty 5s metal orbital (Table VI, Figure 9). The metal 4d$_{xz,yz}$ based (11a$_g$, 8b$_g$) orbitals remain mostly nonbonding in character (Table VI).

The metal d$_{x^2-y^2}$ orbital provides significant contributions to the 8a$_g$, 9a$_g$, and 10a$_g$ MOs mostly because of interactions with the 8a$_g$ (σ_+(P−B)) and 7a$_g$ (σ_+(P−C)) ligand orbitals (Table VI, Figure 8). In practice the 8a$_g$ MO shares comparable contributions also from d$_{z^2}$ and d$_{xz}$ metal orbitals (Table VI) due to π interactions of these metal orbitals with the π_{xz} densities of the 7a$_g$ ligand orbital (Figure 9).

Interactions involving virtual orbitals also represent a source of energetic stabilization for the molecule. Thus 7a$_u$ and 9b$_u$ MOs are significantly admixed with metal 6p orbitals (Table VI, Figure 10) and there is evidence of involvement of the metal 4d$_{xy}$ orbital in the strongly bonding 6b$_g$ MO and, to a smaller extend, in the 7b$_g$ MO (Figure 10). Because of this ligand-to-metal charge transfer the charge on the metal center is reduced to +0.131. Furthermore, the P−C overlap population (Tables I, VI, and VIII) and hence the P−C bond order are both considerably lowered upon coordination.

The ligand (L)⁻ can be classified as a strong, purely σ-donor ligand.[36]

The onset region (up to 9-eV IE) of the PE spectra of the present d⁸ complexes (Figures 11 and 12) differs

Table VII. Relevant PE Data, Computed IEs, and Assignments of the PE Spectra of Pd(L)₂ and Pt(L)₂

band label	IE, eV exptl[a]	ΔSCF[b]	PT[b]	rel intens[c] He I	He II	assgnt[d]
Pd(L)₂						
a	6.85	5.90 (1.92)	6.04 (1.97)	1.21	1.45	12a$_g$
a′	7.05	6.53 (0.99)	6.60 (1.03)	1.00	1.00	7a$_u$
a″	7.32	6.66 (0.99)	6.74 (1.02)	0.99	1.05	9b$_u$
a‴	7.64	6.94 (3.02) / 7.09 (2.82)	6.81 (3.23) / 6.96 (3.03)	2.15	2.80	8b$_g$ / 11a$_g$
b	9.20		10.32 (0.76) / 10.75 (0.38)			9a$_g$ / 8b$_u$
x	9.80	8.80 (2.04)	8.97 (1.92)			10a$_g$
Pt(L)₂						
a	6.45	5.53 (2.18) / 6.08 (2.77)	5.62 (2.24) / 6.06 (2.90)	2.00	2.00	12a$_g$ / 8b$_g$
a′	6.98	6.17 (2.66)	6.16 (2.78)	0.96	0.98	11a$_g$
a″	7.27	6.58 (3.06)	6.56 (3.21)	0.96	1.04	10a$_g$
a‴	7.64	7.10 (0.90) / 7.75 (0.85)	7.20 (0.90) / 7.92 (0.88)	2.30	2.25	7a$_u$ / 9b$_u$
b	9.45		10.69 (0.39) / 10.76 (0.37)			9a$_g$ / 8b$_u$

[a] Experimental IEs refer to deconvoluted Gaussian components. [b] The relaxation energy values are reported in parentheses. PT values represent the relaxation contributions (scaled by a 0.65 factor) to the total reorganization energy (see ref 3). [c] The intensity of bands a′ and a has been taken as reference for Pd(L)₂ and Pt(L)₂, respectively. [d] See Tables VI and VIII for the character of each MO for Pd(L)₂ and Pt(L)₂, respectively.

markedly from those encountered in the previous examples. The spectrum of Pd(L)₂ (Figure 11) consists of a well-defined doublet structure (a, a‴) and of a less well resolved feature a″. Deconvolution has been performed using four asymmetrical Gaussian components whose relative areas are reported in Table VII. In the He II spectrum the components a and a‴ become more intense (Table VII). The higher IE region is similar to those found in the spectra already discussed, even though a new fea-
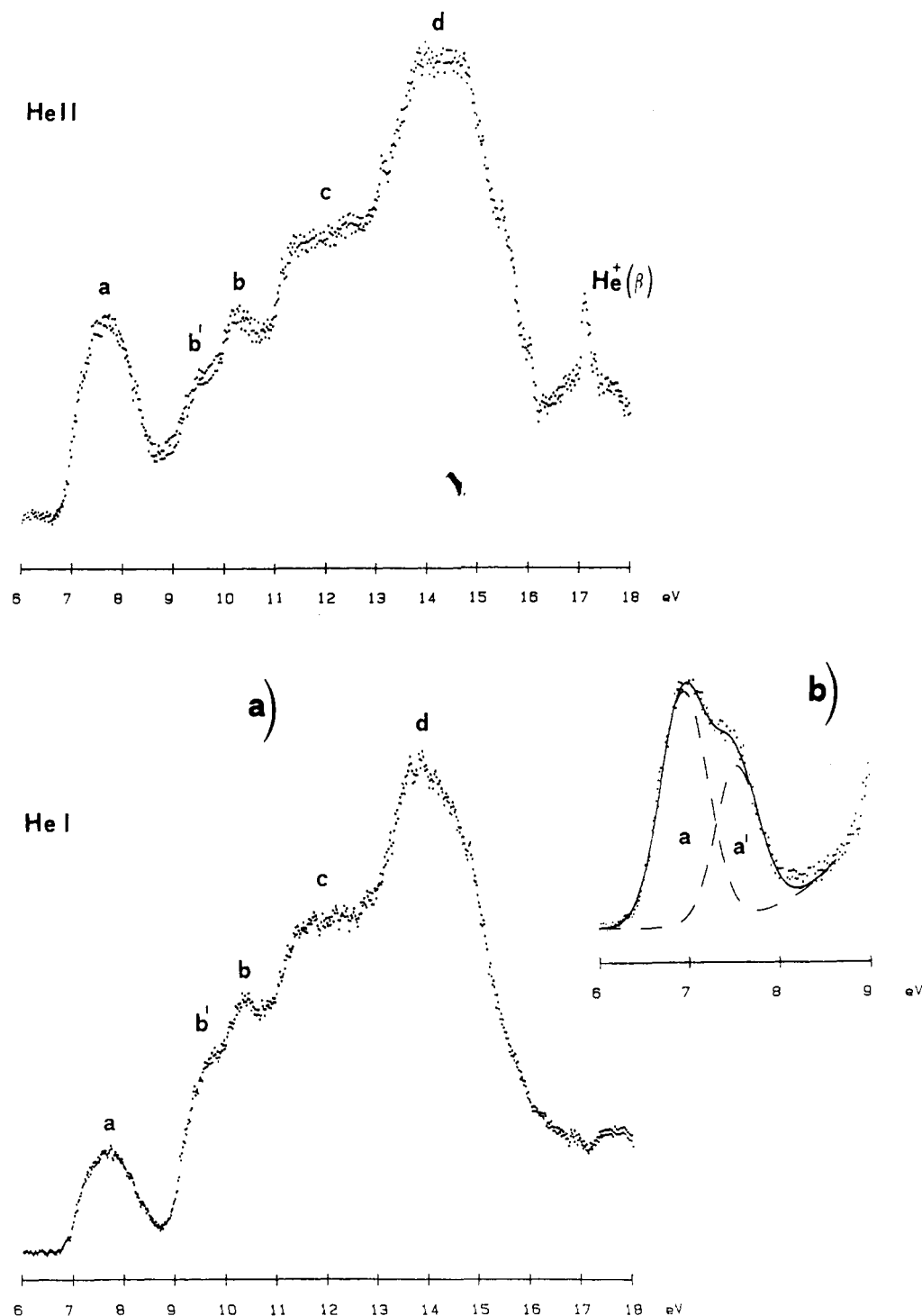
(35) In the diagram only the energies of the valence metal orbitals have been matched in order to reproduce the Pd−C overlap population data. Ab initio eigenvalues of the neutral (L)₂ (rather than (L)₂²⁻) cluster has been used since it better describes the electron distribution in the complexed ligand[3b] whose computed gross charge lies in the present complex around −0.13 eu (see Table VI).

(36) Williams, A. F. *A Theoretical Approach to Inorganic Chemistry*; Springer-Verlag: Berlin, 1979; p 81.

Figure 5. He I and He II spectra of $Be(L)_2$ (a); He I PE spectrum of $Hg(L)_2$ (b), in the low-IE region.

ture, x, appears at 9.80-eV IE.

Computed ΔSCF IEs (Table VII) satisfactorily reproduce the experimental values. Thus, the bands a and a''', more intense in the He II than in the He I spectrum, are assigned to ionization from the $12a_g$ and from $8b_g$ and $11a_g$ MOs. In fact all these orbitals possess a dominant metal d character.[3,13b] The bands a' and a'' represent ionizations from $7a_u$ and $9b_u$ MOs, respectively. Ab initio ΔSCF values (Table VII) would suggest assignments of band b to ionization of the $10a_g$ ($d_{x^2-y^2}$) MO and band x to the $(9a_g)^{-1}$ and $(8b_u)^{-1}$ $(\sigma_+(P-B))$ ionizations. Nevertheless a considerable energy decrease in the latter two ionizations is expected because of the lack of methyls in the calculations. Therefore, it seems reasonable to assign band b to the $(9a_g)^{-1}$ and $(8b_u)^{-1}$ ionizations and the band x, absent in

$Pt(L)_2$ (vide infra), to ionization of the almost fully metal-based $10a_g$ ($d_{x^2-y^2}$) MO.

The He I PE spectrum of $Pt(L)_2$ (Figure 11) presents some analogies with that of its Pd analogue. Worthy of note, however, are (i) a larger energy spread of the a envelope (1.19 vs 0.79 eV in $Pd(L)_2$), (ii) a 2:4 band intensity ratio between the two lower IE main structures (instead of 2:3 observed in the Pd complex, Table VII), (iii) almost no intensity changes on passing to the He II spectrum (Table VII), and (iv) the envelope b does not show the structure that peaks at 9.80 eV (band x) in the spectrum of $Pd(L)_2$.

All these observations together suggest (i) that the ionization of the $5d_{x^2-y^2}$ orbital also contributes to the structure marked a and (ii) that the four ionizations from metal 5d

Table VIII. Ab Initio Eigenvalues and Population Analysis of Outermost MOs of the Model Pt(L)$_2$

MO	eigenvalue, eV	Pt 5d	Pt 6s	Pt 6p	C	P	B	H$_C$	H$_P$	H$_B$	overlap popn Pt–C	dominant character
12a$_g$	7.71	67	25		4	1		1	2		−0.006	d$_{z^2}$
7a$_u$	8.00			2	87	2	1	2	6		0.010	n$_-$
9b$_u$	8.60			2	86	2	2	2	6		0.014	n$_+$
11a$_g$	8.83	85			3	6	1	2	3		−0.036	d$_{xz}$
8b$_g$	8.85	90			2	6		1	1		−0.016	d$_{yz}$
10a$_g$	9.64	90			3	2		3	2		−0.036	d$_{x^2-y^2}$
9a$_g$	10.99	1			1	25	33		11	29	0.002	σ$_+$(P–B)
8b$_u$	11.04				2	25	31		14	28	0.000	σ$_+$(P–B)
7b$_g$	11.59	23			25	27	10	1	14		0.068	n$_-$, d$_{xy}$
6a$_u$	12.09				7	60	24	2	7		0.000	σ$_-$(P–B)
7b$_u$	12.25				19	15	31	4	5	26	0.000	σ$_+$(P–C)
8a$_g$	12.39	9	3		18	11	30	2	2	25	0.012	σ$_+$(P–C), d$_{xz}$ (65%), d$_{z^2}$ (35%)
6b$_g$	12.41	19			25	40	13	2	1		0.052	σ$_-$(P–B), d$_{xy}$
7a$_g$	12.87	21	11		36	5	4	3	12	6	0.104	d$_{z^2}$, n$_+$
5a$_u$	13.30				35	36		13	16		0.000	σ$_-$(P–C)
5b$_g$	13.51	5			31	32		12	20		0.012	σ$_-$(P–C)

Atomic Charge

Pt	C	P	B
+0.080	−0.302	+0.052	+0.112

Overlap Population

Pt–C	P–C	P–B
0.360	0.610	0.413

Metal Orbital Population

| 6s	6p$_x$	6p$_y$	6p$_z$	5d$_{x^2-y^2}$	5d$_{z^2}$	5d$_{xy}$	5d$_{xz}$	5d$_{yz}$
0.936	0.068	0.063	0.021	1.976	1.860	1.065	1.968	1.963
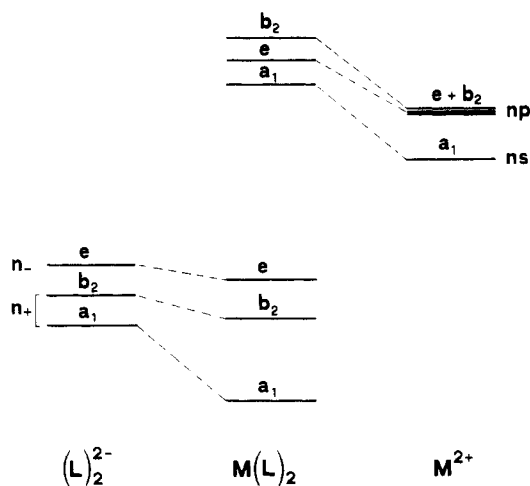
Figure 6. Qualitative MO diagram of uppermost MOs for M(L)$_2$ (M = Be, Cd, Hg) complexes in D_{2d} symmetry.
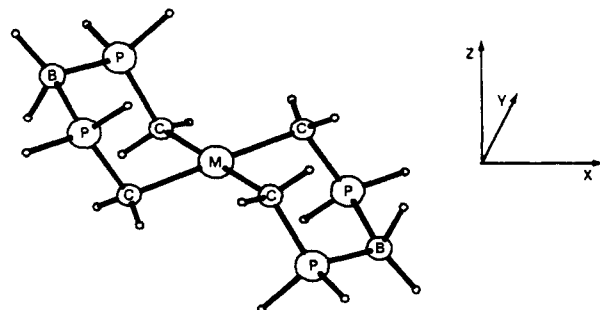
Figure 7. Geometry and choice of axes for the model M(L)$_2$ (M = Ni, Pd, Pt) complexes.

based orbitals are spread inside the main low-IE structure.

Ground-state ab initio data of Pt(L)$_2$ (Table VIII) are similar to those of its Pd analogue. The differences seem
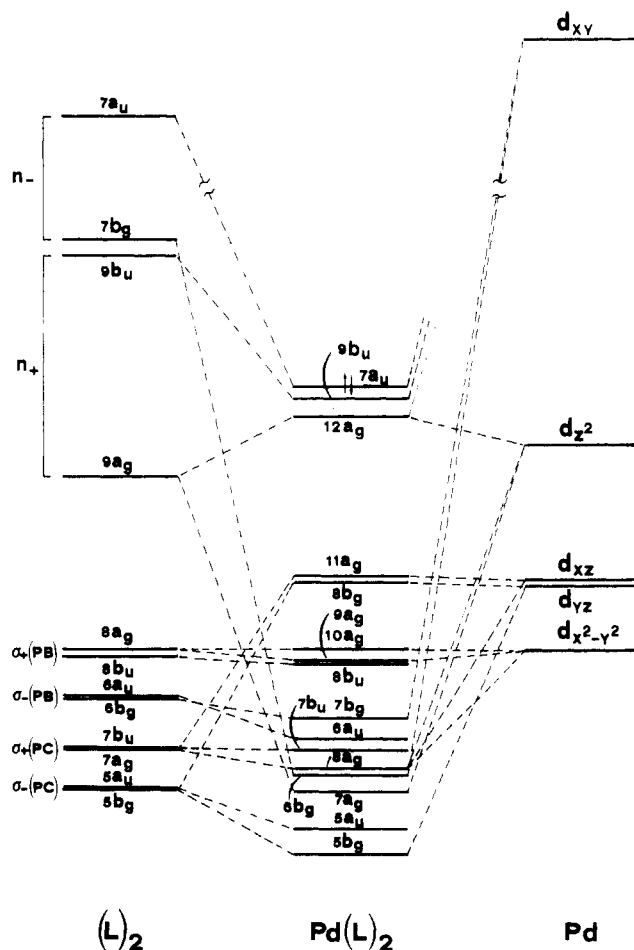
Figure 8. Molecular orbital scheme of Pd(L)$_2$.

to be due to a minor metal–ligand orbital admixture (Table VIII) as well as to the expected upward shift of orbital
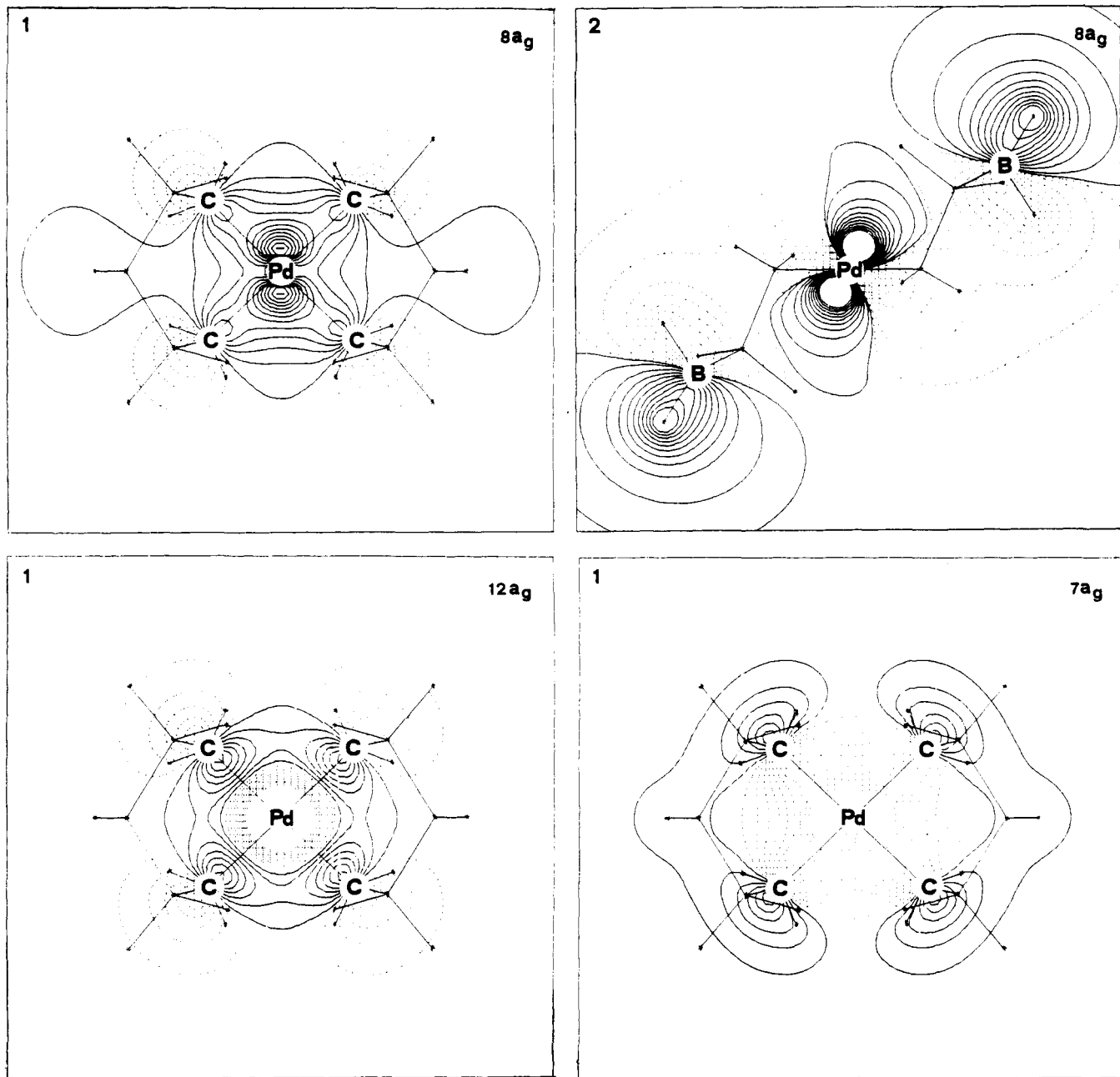
Figure 9. Wave function contour plots of the model Pd(L)$_2$ for the $7a_g$, $8a_g$, and $12a_g$ MOs: view 1, xy plane through C-Pd-C bonds; view 2, xz plane through the Pd and two B atoms. Each set of contours is drawn in a frame of 10 × 10 au, and the stars indicate projections of each atom on the contour plane. Contours interval as in Figure 2.

energies associated with metal 5d subshells.[3,13a] Therefore for Pt(L)$_2$ the MOs having dominant metal 5d character coalesce in a narrower energy range than the Pd complex (Table VIII). It is noted, in addition, that the $7a_u$ and $9b_u$ MOs are clearly more tightly bound (Table VIII). This effect seems to be due to operation of smaller interligand interaction (bonding in the case of $7a_u$ and antibonding for the $9b_u$; Figure 10), due to the larger metal-ligand distance.

Relaxation energies associated with production of nominally "$5d^{-1}$ ion states" (Table VII) upset the sequence of ground-state MOs energies and result in a "classical" sequence of uppermost lying ^2D states, namely, $d_{z^2} < d_{yz} \simeq d_{xz} < d_{x^2-y^2}$. Assignment is therefore straightforward. Band a is due to ionizations of the $12a_g$ (d_{z^2}) and $8b_g$ (d_{yz}) MOs, whereas bands a' and a'' arise from ionizations of the $11a_g$ (d_{xz}) and $10a_g$ ($d_{x^2-y^2}$) MOs, respectively. The remaining band a''' corresponds to the the ligand-based $9b_u$ (n_+) and $7a_u$ (n_-) MOs.

It is also noted that, despite the remarkable contribution of metal 5d subshells to MOs associated to bands a, a', and a'', no He I/He II intensity variation was observed relative to the next band, a''' (Table VII). Recent experimental PE measurements on alkyl complexes of Pt[37] have, however, shown no He I/He II band intensity changes in the metal 5d ionizations.

Finally, some comments are required for Ni(L)$_2$. The PE spectrum is shaped differently in the lower IE region from those of Pd(L)$_2$ and Pt(L)$_2$. Two well-separated structures are observed up to 8-eV IE (Figure 12). With He II radiation, the structure a–a' becomes prominent relative to a'', b, and c, thus suggesting that a and a' are due to production of $3d^{-1}$ ion states. The higher IE region

(37) Yang, D.-S.; Bancroft, G. M.; Bozek, J. D.; Puddephatt, R. J. *Inorg. Chem.* **1989**, *28*, 2. Yang, D.-S.; Bancroft, G. M.; Puddephatt, R. J.; Bursten, B. E.; McKee, S. D. *Inorg. Chem.* **1989**, *28*, 872 and references therein.

9b_u

7a_u

6b_g

7b_g
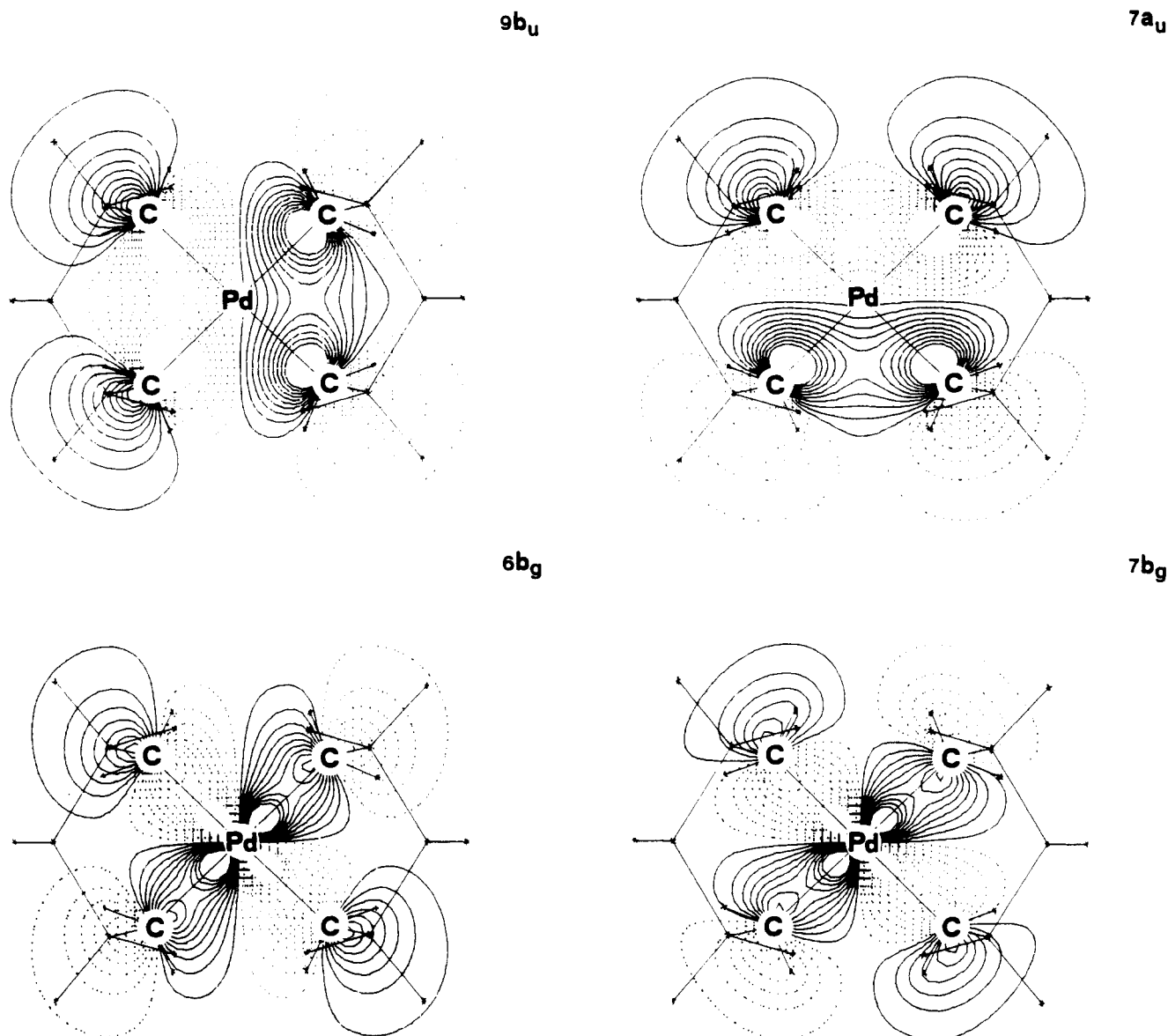
Figure 10. Wave function contour plots of the model Pd(L)$_2$ for the 6b$_g$, 7b$_g$, 9b$_u$, and 7a$_u$ MOs in the xy plane through C-Pd-C bonds. Each set of contours is drawn in a frame of 10 × 10 au, and the stars indicate projections of each atom on the contour plane. Contours interval as in Figure 2.

up to 11 eV is similar to that of previously discussed spectra.

Ab initio calculations provide a suitable rationale of the ground-state electronic structure. The ligand localized MOs have an energy similar to those of the Pd and Pt complexes and MOs having predominantly metal d character are considerably more tightly bound (supplementary material; see paragraph at end of paper). The assignment, however, based on ΔSCF IEs does not fit experimental values or the relative intensity data. Relaxation energies associated to nominally "3d^{-1} ion states" are not large enough to result in uppermost lying ^{2}D states. This is not surprising, since it is well-known that differential correlation energy problems associated with electronic states of the nickel atom[38] may invalidate any SCF ab initio description of ground and ionic states of nickel-containing molecules.[39,40]

**Table IX. Experimental IEs and Assignment of the PE Spectrum of Ni(L)$_2$**

band label	IE, eV	assgnt
a	6.00	3d metal-based
a'	6.41	3d metal-based
a''	7.40	7a$_u$ (n_-), 9b$_u$ (n_+)
b	8.95	σ_+(P-B)

An assignment can however be put forward on a purely experimental basis (Table IX). On the basis of He I/He II intensity changes, the envelope a-a' can be safely associated to ionizations of at least three 3d metal-based MOs. Present data available do not allow an unambiguous assessment of whether the band includes the fourth 3d^{-1} ionization or of whether, perhaps, that ionization is included in the poorly resolved envelope between 8 and 10.5

(38) Martin, R. L. *Chem. Phys. Lett.* **1980,** *75,* 290. Botch, B. H., Jr.; Dunning, T. H.; Harrison, J. F. *J. Chem. Phys.* **1981,** *75,* 3466. Bausch-licher, C. W., Jr.; Walch, S. P.; Partridge, H. *J. Chem. Phys.* **1982,** *76,* 1033.

(39) von Niessen, W.; Cederbaum, L. S. *Mol. Phys.* **1981,** *43,* 897. Moncrieff, D.; Hillier, I. H.; Saunders, V. R.; von Niessen, W. *Inorg. Chem.* **1985,** *24,* 4247.

(40) Ciliberto, E.; Di Bella, S.; Fragalà, I.; Granozzi, G.; Burton, N. A.; Hillier, I. H.; Guest, H. F.; Kendrick, J. *J. Chem. Soc., Dalton Trans.* **1990,** 849.
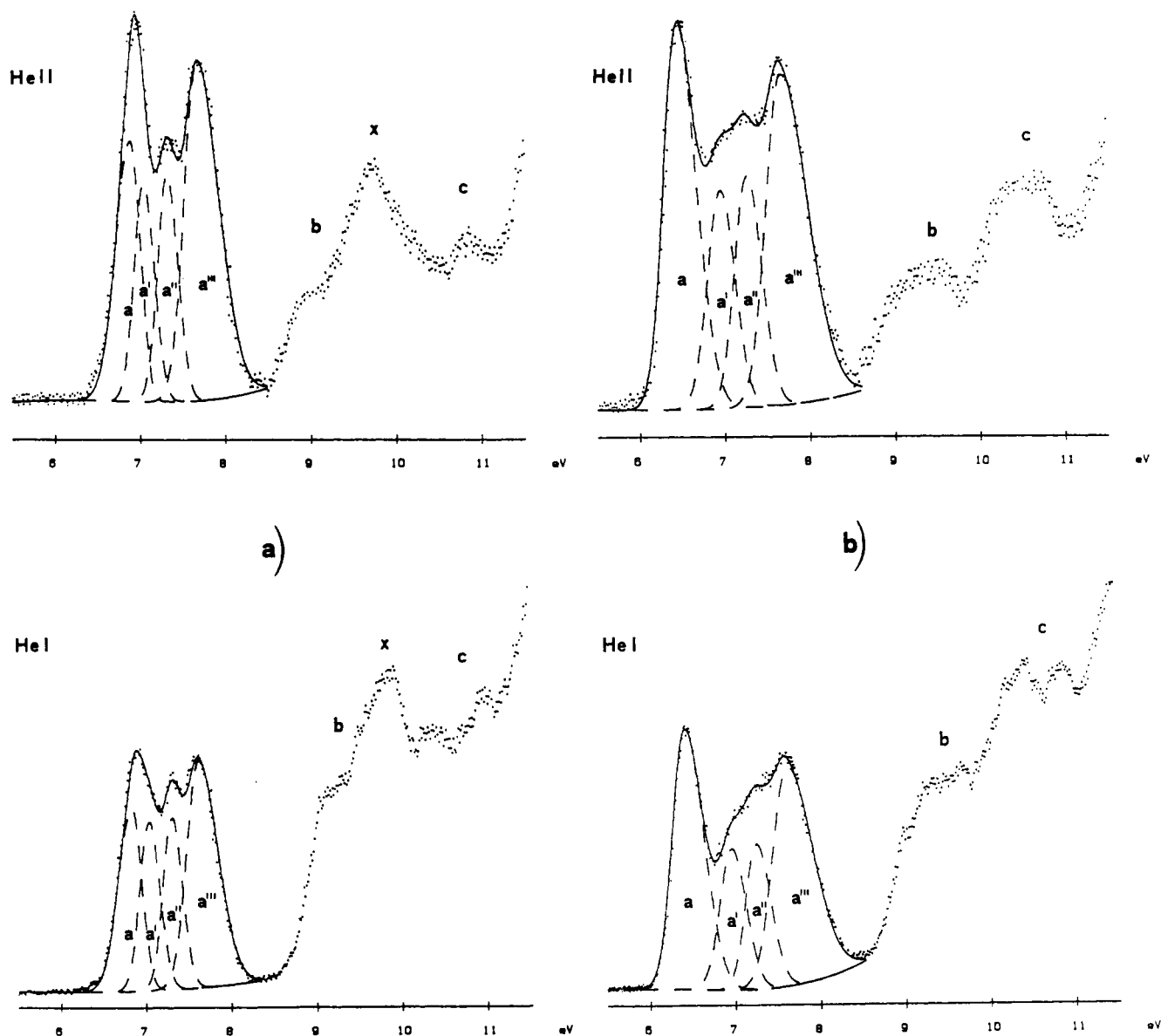
Figure 11. He I and He II PE spectra of Pd(L)₂ (a) and Pt(L)₂ (b) in the low-IE region: experimental spectrum (point lines), Gaussian components (dashed lines), convolution of Gaussian (solid line).

eV IE. The next band a″, on the basis of previous spectra, is assigned to ionization of $7a_u$ (n_-) and $9b_u$ (n_+) MOs since it falls in the expected IE region. Finally, the band b, whose intensity falls off in the He II spectrum, can be associated with ionization of σ_+(P–B) MOs.

Concluding Remarks

This paper presents a comprehensive study of the electronic structure of some phosphorus ylide homo- and heteroleptic complexes of various metal ions that include main-group metals as well as transition metals. Despite its intriguing nature, the present ligand displays bonding properties that are nearly comparable with those of less exotic hydrocarbyl ligands, thus allowing comparative argumentations.

The chemistry of homoleptic σ-bonded hydrocarbyls has been extensively reviewed,[41] and structural, kinetic, and thermodynamic factors favoring relative stabilities have been widely discussed from both theoretical[42,43] and ex-

perimental viewpoints.[44,45] Classical alkyl ligands often form coordinatively unsaturated environments around the metal ions. They contribute one electron to the valence shell and therefore neutral alkyl complexes of the main-group metal ions do not fulfill both coordination and electron stability requirements and thus result in extended oligo–polymeric bridged structures or in anionic species.[41] Transition metal–alkyl chemistry also deserves detailed attention. Metal d^0 hydrocarbyls have tetrahedral or octahedral geometries.[41] They do not fulfill the 18-electron rule but, like main-group metal complexes, have filled bonding valence orbitals consisting of combinations of formal σ(M–C) bond orbitals.[46] d^n ground-state configu-

(41) (a) Davidson, P. J.; Lappert, M. F.; Pearce, R. *Chem. Rev.* **1976,** *76,* 219; *Acc. Chem. Res.* **1974,** *7,* 209. (b) Schrock, R. R.; Parshall, G. W. *Chem. Rev.* **1976,** *76,* 243.

(42) Low, J. J.; Goddard, W. A., III *J. Am. Chem. Soc.* **1986,** *108,* 6115. Low, J. J.; Goddard, W. A., III *Organometallics* **1986,** *5,* 609.
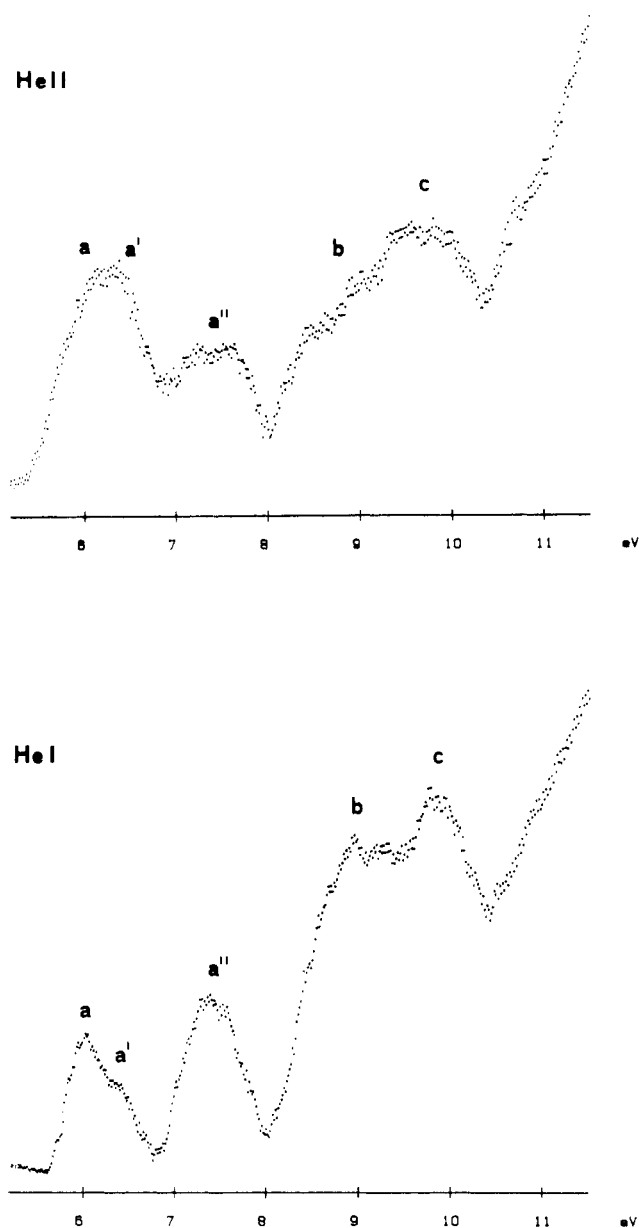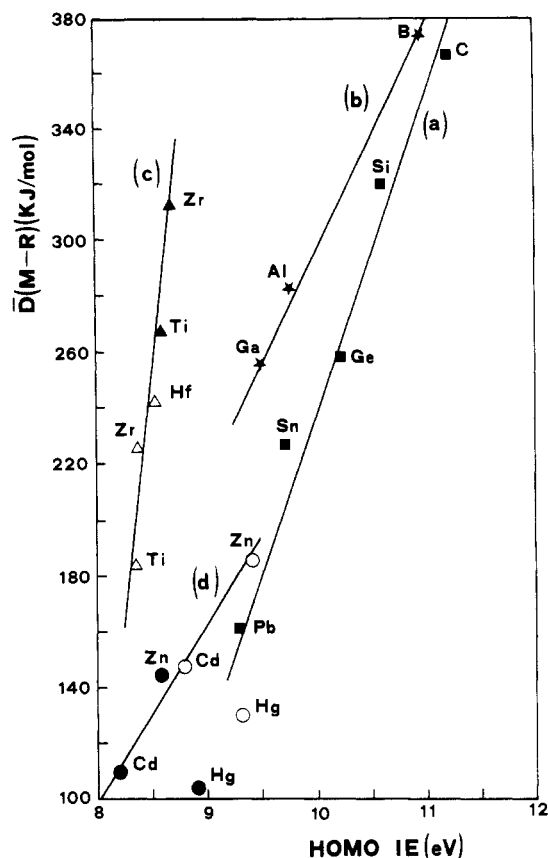
(43) Ziegler, T.; Tschinke, V.; Becke, A. *J. Am. Chem. Soc.* **1987,** *109,* 1351. Schilling, J. B.; Goddard, W. A., III; Beauchamp, J. L. *J. Am. Chem. Soc.* **1987,** *109,* 5573. Ziegler, T.; Cheng, W.; Baerends, E. J.; Ravenek, W. *Inorg. Chem.* **1988,** *27,* 3458. Bauschlicher, C. W.; Langhoff, S. R.; Patridge, H.; Barnes, L. A. *J. Chem. Phys.* **1989,** *91,* 2399.

(44) Cowley, A. H. *Prog. Inorg. Chem.* **1979,** *26,* 45.

(45) Halpern, J. *Acc. Chem. Res.* **1982,** *15,* 238.

(46) Lappert, M. F.; Pedley, J. B.; Sharp, G. *J. Organomet. Chem.* **1974,** *66,* 271.

He II

He I

Figure 12. He I and He II PE spectra of $Ni(L)_2$ in the low-IE region.

Figure 13. Correlation between $\bar{D}(M-R)$ and HOMO IEs values for selected hydrocarbyl complexes: ■, MR_4 (R = Me)[47a,27a] (a); ✱, MR_3 (R = Me)[47a,29] (b); O, MR_2 (R = Me),[47a,48] ●, MR_2 (R = Et)[47a,48] (c); △, MR_4 (R = CH_2CMe_3),[47b,46] ▲, MR_4 (R = CH_2SiMe_3)[47b,46] (d). The lines represent least-squares fits to the data points.

rations are also generally observed in connection with the lower oxidation state of the complexed metals. In any case, coordinatively demanding metals become stable only in the presence of bulky ligands which crowd the coordination sphere.[41] Otherwise oligomerization–polymerization of low-coordination number subunits occurs, or the presence of an ancillary, π-acceptor, ligand is often required.[41] Complexes of monofunctional or difunctional ylides can be generally discussed in a similar way.

The present phosphorus ylide complexes readily form metal-to-carbon σ-alkyl bonds, and their chemistry can be more readily accounted for by a naive chemical intuition. The ligand contributes three electrons to the counting. Because of the chelating nature, it saturates two coordination sites and thus favors lower oxidation states and higher coordination numbers of the bonded metal.[1] Their chemistry, therefore, consists of monomeric pseudotetrahedral complexes of group II and III metals in the +2 or +3 oxidation states, and tetracoordinated $M(L)_2$ complexes in the usual tetrahedral (M = Mn) or square-planar (M = Ni, Pd, Pt, Au) coordination environments.[1] Metal +3 octahedral complexes have not been reported as yet. These

complexes all possess completely filled valence orbitals representing combinations of σ(M–C) bond orbitals (vide infra). In the case of Ni-triad complexes, stable "16-electron" species are formed without any ancillary ligands. Thermochemical data are not available for the present complexes, and therefore any direct comparison of the strength of the metal–carbon bond relative to classical alkyls cannot be made. Nevertheless, the presently observed trends of IE values might be informative. Reliable literature data on various metal–alkyl complexes indicate that there is a linear dependence between mean bond dissociation energies[47] ($\bar{D}(M-R)$) and HOMO IE values[27a,29,46,48] taken from PE spectra (Figure 13). It appears that the higher the HOMO IE value, $\bar{D}(M-R)$ will be correspondingly larger. Extension of this observation to the present ylide complexes does not appear straightforward since only a few of mentioned data refer to a suitable homogeneous series of the same metal ions. As a matter of fact, extrapolation of the linear relationship observed for two groups of Cd and Hg alkyls (Figure 13d) to the present $M(L)_2$ (M = Cd, Hg) complexes would lead to counterintuitively smaller $\bar{D}(M-R)$ energies, which would contrast with their known chemical robustness.

In this context, however, two observations must be made. First, the IE values associated with $3d^{10}$ ionizations are lower in $(CH_3)_2Ga(L)$ (Table III) than in the $Ga(CH_3)_3$

(47) (a) Pilcher, G.; Skinner, H. A. In *The Chemistry of the Metal–Carbon Bond*; Hartley, F. R., Patai, S., Eds.; Wiley: New York, 1982; Chapter 2. (b) Skinner, H. A.; Connor, J. A. *Pure Appl. Chem.* **1985**, *57*, 79.

(48) Creber, D. K.; Bancroft, G. M. *Inorg. Chem.* **1980**, *19*, 643.

complex[31b] and, since these data are a sensible measure of the ligand capability of increasing or depleting electron density on the metal center,[49] the ligand L represents a considerably stronger electron donor than alkyls. Second, the IE values associated with ionization of valence MOs representing $\sigma(M-C)$ bonds in the present group II and III metal complexes are almost generally the lowest yet observed among metal hydrocarbyls.[29,48,50] In accordance with reported IE measurements of alkyl radicals[51] and of various phosphorus ylide systems,[15b,c] this might be due, to first order, to a greater energy value (ϵ_L) associated with unperturbed ylide lone pairs than found with simpler alkyl groups. Furthermore, the ϵ_L value may be modulated by the orbital interaction energy (ΔE) given by the approximate expression[23]

$$\Delta E = -\frac{K\langle\psi_L|\psi_M\rangle^2}{\epsilon_L - \epsilon_M} \qquad (1)$$

where K is a constant, ϵ_L and ϵ_M are the ligand and the metal interacting orbitals having ϵ_L and ϵ_M eigenvalues,[23] and $\langle\psi_L|\psi_M\rangle$ is the overlap integral.

Therefore, given comparable $\langle\psi_L|\psi_M\rangle$ terms for both alkyl and ylide complexes of the same metal (comparable angular dependence of wave functions and M–L distances), it transpires that smaller $\epsilon_L - \epsilon_M$ terms and, hence, larger ΔE values must be expected for the former complexes. This qualitative anticipation of larger metal–ligand interactions in the present ylide complexes finds a tuned counterpart in the present data for the $(CH_3)_2M(L)$ (M = Al, Ga) complexes that represent an ideal case of an "internal reference" model. In fact, the greater stabilization of those MOs which represent the $\sigma(M-C_{yl})$ bonds (relative

to $\sigma(M-C_{meth})$) (Table II) must certainly be associated with the better ($\epsilon_L - \epsilon_M$) energy matching.

The description of the metal–ligand bonding of homoleptic d^8 metal $M(L)_2$ complexes appears to be much more intriguing. The metal d subshells lead to severe perturbations of ligand ylidic lone pairs. Mulliken populations are indicative of a s^1d^9 configuration as was indicated by GVB calculations on $M(CH_3)_2(PR_3)_2$ complexes (M = Pd, Pt).[42] The metal–ligand bonding is strongly dominated by σ interactions almost involving virtual metal orbitals, even though some π interactions involve the more internal ligand $\sigma_+(P-B)$ and $\sigma_+(P-C)$ MOs and the metal $nd_{x^2-y^2}$ orbital.

From a purely spectroscopic point of view, the present PE spectra have been discussed and interpreted on the basis of ab initio ΔSCF calculations. This approach, however, failed in the case of nickel complex possibly due to differential correlation problems associated to production of d^{-1} ionic states.[38-40] The PE spectra have been, thus, interpreted on a purely experimental basis. Further work is, however, in progress using ab initio Greens function calculations.[52]

Supplementary Material Available: A listing of ground-state ab initio data for $Ni(L)_2$ (1 page). Ordering information is given on any current masthead page.

(49) Bursten, B. E.; Green, M. R. *Prog. Inorg. Chem.* 1988, *36*, 393.
(50) Böhm, M. C.; Gleiter, R.; Morgan, G. L.; Lusztyk, J.; Starowieyski, K. B. *J. Organomet. Chem.* 1980, *194*, 257.
(51) Schultz, J. C.; Houle, F. A.; Beauchamp, J. L. *J. Am. Chem. Soc.* 1984, *106*, 3917.

(52) Di Bella, S.; Fragalà, I.; Hillier, I. H. Work in progress.